Effect of Environmental Factors on the Kinetics of Insulin Fibril Formation: Elucidation of the Molecular Mechanism†

Liza Nielsen,‡ Ritu Khurana,‡ Alisa Coats,‡ Sven Frokjaer,§ Jens Brange,||,⊥ Sandip Vyas,‡ Vladimir N. Uversky,‡ and Anthony L. Fink*,‡

Department of Chemistry and Biochemistry, University of California, Santa Cruz, California 95064, Department of Pharmaceutics, The Royal Danish School of Pharmacy, 2100 Copenhagen, Denmark, and Novo Nordisk A/S, Novo Alle, 2880 Bagsvaerd, Denmark

Received November 6, 2000; Revised Manuscript Received March 20, 2001

ABSTRACT: In the search for the molecular mechanism of insulin fibrillation, the kinetics of insulin fibril formation were studied under different conditions using the fluorescent dye thioflavin T (ThT). The effect of insulin concentration, agitation, pH, ionic strength, anions, seeding, and addition of 1-anilinonaphthalene-8-sulfonic acid (ANS), urea, TMAO, sucrose, and ThT on the kinetics of fibrillation was investigated. The kinetics of the fibrillation process could be described by the lag time for formation of stable nuclei (nucleation) and the apparent rate constant for the growth of fibrils (elongation). The addition of seeds eliminated the lag phase. An increase in insulin concentration resulted in shorter lag times and faster growth of fibrils. Shorter lag times and faster growth of fibrils were seen at acidic pH versus neutral pH, whereas an increase in ionic strength resulted in shorter lag times and slower growth of fibrils. There was no clear correlation between the rate of fibril elongation and ionic strength. Agitation during fibril formation attenuated the effects of insulin concentration and ionic strength on both lag times and fibril growth. The addition of ANS increased the lag time and decreased the apparent growth rate for insulin fibril formation. The ANS-induced inhibition appears to reflect the formation of amorphous aggregates. The denaturant, urea, decreased the lag time, whereas the stabilizers, trimethylamine *N*-oxide dihydrate (TMAO) and sucrose, increased the lag times. The results indicated that both nucleation and fibril growth were controlled by hydrophobic and electrostatic interactions. A kinetic model, involving the association of monomeric partially folded intermediates, whose concentration is stimulated by the air−water interface, leading to formation of the critical nucleus and thence fibrils, is proposed.

Physical and chemical instability problems are among the most challenging tasks in development of protein delivery systems (*1*). The most common physical stability problem is protein aggregation or fibril formation. Insulin has been used for more than 75 years in the treatment of insulin-dependent diabetic patients, but much effort is still being spent to improve and optimize the therapeutic use of insulin. Studying the kinetics and identifying the key steps in the formation of insulin fibrils may reveal important information for prevention of fibril formation. Furthermore, it may help elucidate the mechanism for the development of a number of neurodegenerative disorders such as Alzheimer's disease, Parkinson's disease, and bovine spongiform encephalopathy, which are all characterized by an abnormal protein deposition (*2*−*4*).

Insulin is normally formulated as a zinc-coordinated hexamer, which is the physiologically predominant form. The hexamer is formed by the association of three dimers, and is stabilized by two to four zinc ions. Zinc-free insulin is a dimer at low protein concentrations over the pH 2−8 range, shifting to a tetramer at protein concentrations of >1.5 mg/mL. Insulin is conformationally very stable under acidic conditions at ambient temperatures (*5*). In 20% acetic acid, insulin is monomeric (*6*, *7*).

Formation of insulin fibrils is a physical process in which non-native insulin molecules interact with each other to form linear, biologically inactive aggregates (*8*). It was recognized, early, that three reactions are involved in fibril formation: nucleation (formation of stable nuclei), growth (elongation of nuclei to fibrils), and precipitation (floccule formation) (*9*, *10*). Nucleation required temperatures above ambient, whereas growth into fibrils also occurred at ambient or lower temperatures (*10*). In agreement with these observations, fibril formation has later been described by a nucleation-dependent elongation mechanism involving three phases, nucleation, elongation, and an equilibrium phase (*11*−*14*). Nucleation is viewed as the assembly of several protein monomers to form an organized structure, the nucleus, as a precursor for formation of fibrils. Subsequent addition of monomers to the nucleus elongates it into fibrils (*14*). This

† This research was supported by the Academy of Technical Sciences (ATV) in Denmark and a grant from the University of California BioSTAR program.

* To whom correspondence should be addressed: Department of Chemistry and Biochemistry, University of California, Santa Cruz, CA 95064. Phone: (831) 459-2744. Fax: (831) 459-2935. E-mail: enzyme@cats.ucsc.edu.

‡ University of California.

§ The Royal Danish School of Pharmacy.

|| Novo Nordisk A/S.

⊥ Current address: Brange Consult, Krøyersvej 22C, 2930 Klampenborg, Denmark.

10.1021/bi002555c CCC: $20.00
Published on Web 04/24/2001

model has been found to apply for fibrillation of several proteins, including Alzheimer's amyloid β-peptide (*13*), a peptide derived from OsmB resembling the C-terminal region of amyloid β-protein (*11*), and α-synuclein (*15*).

The driving force for insulin aggregation is assumed to be hydrophobic in nature. It has been suggested that the initial step is the exposure of certain hydrophobic residues, normally buried in the three-dimensional structure, to the surface of the insulin monomer. Thus, the initial step in aggregation is probably the formation of monomeric, conformationally changed molecules, in which the hydrophobic faces, normally buried in the dimer and hexamer, become exposed to solvent (*16*, *17*). Insulin has a very strong propensity to form fibrils in the presence of hydrophobic surfaces, including the air−water interface formed on agitation (*18*, *19*). Amyloid deposits have been observed both in patients with type II diabetes (*20*−*22*) and in normal aging (*23*), as well as after continuous subcutaneous insulin infusion (*24*) and after repeated insulin injections (*25*). However, the major problem with insulin aggregation is in the production, storage, and delivery of the protein. For example, fibril formation is a major problem in the commercial isolation and purification steps, where many steps in the purification of insulin involve a pH of 1−3. The low pH promotes relatively rapid fibril formation (*26*). Agitation of insulin solutions during transportation, and in portable delivery systems, also triggers aggregation (*18*).

Quantitative analysis of the kinetics of fibril formation requires both well-characterized protein preparations and appropriate monitoring techniques, as significant variations in the degree of aggregation in the initial solutions may lead to large experimental irreproducibility. Several techniques have been employed in the study of fibrillation of proteins, including quasielastic light scattering, turbidity, analytical ultracentrifugation, size exclusion chromatography, transmission electron microscopy, and atomic force microscopy (*11*, *27*−*31*).

The histological dye thioflavin T (ThT)[1] has been widely used for the detection of amyloid fibrils (*32*, *33*). In the presence of fibrils, ThT gives rise to a new excitation maximum at 450 nm and enhanced emission at 482 nm, whereas unbound ThT is essentially nonfluorescent at these wavelengths. Insulin fibrils have been shown to fluoresce intensively with ThT, resulting in fluorescent properties that are indistinguishable from those of other amyloid fibrils (*33*, *34*). ThT is believed to interact relatively specifically and rapidly with amyloid fibrils, and the binding is independent of the primary structure of the protein (*34*). Only the multimeric fibrillar forms, not multiple β-sheet domains in native proteins, fluoresce with ThT. Measuring the level of binding of ThT to insulin fibrils is thus a potential powerful tool for studying the kinetics of insulin fibril formation (*35*). Insulin fibril formation has been shown to result in formation of β-sheet structure (*36*, *37*).

The purpose of this paper was to study the kinetics of insulin fibril formation by investigating the effect of insulin concentration, agitation, pH, ionic strength, anions, seeding, and addition of 1-anilinonaphthalene-8-sulfonic acid (ANS), urea, trimethylamine *N*-oxide dihydrate (TMAO), sucrose, and ThT on the fibrillation process, and thereby gain more insight into the molecular mechanism of insulin fibril formation.

[1] Abbreviations: AFM, atomic force microscope; ANS, 1-anilinonaphthalene-8-sulfonic acid; CD, circular dichroism; k_{app}, apparent rate constant for fibril growth (elongation rate); ThT, thioflavin T; TMAO, trimethylamine *N*-oxide dihydrate.

MATERIALS AND METHODS

Materials. Monocomponent (MC) bovine insulin (batch 96o1331) was obtained from Novo Nordisk A/S. The zinc content of insulin was 0.4% (w/w of insulin), corresponding to approximately two Zn^{2+} ions per insulin hexamer. Thioflavin T, 1-anilinonaphthalene-8-sulfonic acid, and trimethylamine *N*-oxide dihydrate were obtained from Sigma (St. Louis, MO). All other chemicals were of analytical grade from FisherChemicals.

Preparation of Insulin Fibrils. All insulin samples were made from a fresh stock solution of 20 mg/mL (~3.5 mM) bovine insulin in 0.04 M HCl (pH 1.6) prepared immediately prior to each experiment. This was done to minimize the possible formation of nuclei in an old stock solution, which would affect the kinetics of fibril formation. For the concentration dependency study, the insulin stock solution was diluted in 0.025 M HCl and 0.1 M NaCl (pH 1.6) to obtain concentrations ranging from 0.2 to 20 mg/mL. The insulin concentration was measured by UV absorption at 276 nm using an extinction coefficient of 1.0 for 1.0 mg/mL (*38*).

The effect of anions was studied using an insulin concentration of 2 mg/mL in 0.025 M HCl (pH 1.6) with concentrations of NaCl, Na_2SO_4, and NaH_2PO_4 ranging from 0.05 to 0.50 M. The effect of acids, hydrochloric acid, sulfuric acid, and phosphoric acid, was studied using 2 mg/mL insulin in 0.025−0.50 M HCl, 0.0167−0.50 M H_2SO_4, and 0.1−0.5 M H_3PO_4 with a pH between 0.5 and 1.7. These experiments were carried out using in situ ThT fluorescence as described below.

The effect of pH, ANS, and ThT on the kinetics of insulin fibrillation was studied in glass vials. For studying the effect of pH, 1 mg/mL bovine insulin was dissolved in 0.025 M HCl and 0.1 M NaCl at pH 1.6, 20 mM formate buffer and 0.1 M NaCl at pH 3, and 20 mM phosphate buffer and 0.1 M NaCl at pH 7.4. The effect of ANS was studied using 1 mg/mL (0.17 mM) insulin dissolved in 0.1 M HCl (pH 1.6) using a molar ratio of 10:1 (1.8 mM ANS) and 50:1 (9 mM ANS). A 1 mg/mL insulin solution in 0.1 M HCl (pH 1.6) without ANS was used as a control. Each sample (0.5 mL) was incubated at 37 °C in 1.8 mL borosilicate glass vials with rubber-lined closures (from Fisherbrand). The solutions were stirred with micro stirring bars (8 mm × 1.5 mm) from Fisherbrand. At appropiate time intervals, the vial was gently shaken to distribute fibrils evenly in the vial before withdrawing aliquots of 10 μL. The effect of ThT on the kinetics of insulin fibril formation was also studied in glass vials by incubating 1 mg/mL insulin solutions in 0.0225 M HCl and 0.0775 M NaCl (pH 1.6) with and without 20 μM ThT and removing aliquots for fluorescence measurements.

The effect of urea, trimethylamine *N*-oxide dihydrate (TMAO), and sucrose on the kinetics of insulin fibrillation was studied by incubating the samples in 96-microwell polystyrene plates at 43 °C without agitation. Bovine insulin (2 mg/mL) was dissolved in 20 mM phosphate buffer and 0.1 M NaCl (pH 7.4), and urea was added at concentrations

of 2, 4, and 6 M. The effect of the stabilizers, TMAO and sucrose, was studied under monomeric conditions, i.e., 20% acetic acid. Bovine insulin (2 mg/mL) was dissolved in 20% acetic acid and 0.1 M NaCl (pH 1.6), and TMAO and sucrose were added at concentrations of 1 M and 10%, respectively.

Preparation of Seeds. The effect of seeding on the kinetics of insulin fibrillation was studied by adding different amounts of preformed fibrils. Bovine insulin (2 mg/mL) was dissolved in 0.025 M HCl and 0.1 M NaCl (pH 1.6). The solution was incubated at 37 °C with stirring for 7 h and subsequently mildly sonicated for 5 min. Aliqouts of 100, 50, 10, and 5 μL were withdrawn and added to 900, 950, 990, and 995 μL, respectively, of a fresh 2 mg/mL bovine insulin solution in 0.025 M HCl and 0.1 M NaCl (pH 1.6). The samples were incubated in a 96-microwell plate at 43 °C without agitation using in situ ThT fluorescence.

Thioflavin T Fluorescence Assays for Fibrillation. A stock solution of ThT was prepared at a concentration of 1 mM in double-distilled water and stored at 4 °C protected from light to prevent quenching until it was used. For in situ ThT fluorescence measurements, 20 μM ThT was added to each of the insulin solutions to be incubated in the 96-microwell polystyrene plates with flat bottoms (Nunc). A sample volume of 200 μL was added to each well. Five replicates corresponding to five wells were measured for each sample to minimize the well-to-well variation. The plates were covered by ELAS septum sheets (Spike International, Ltd.) and incubated at 60 °C without agitation or shaking. The plates were removed from the incubation at 60 °C every 30 min, and fluorescence measurements were performed on a Perkin-Elmer LS 50B spectrofluorometer using the plate reader (excitation at 450 nm, emission at 482 nm). Both the excitation and the emission slits were maintained at 2.5 nm. The read time for each well was 1 s, and the total read time for the whole plate was approximately 3 min. Alternately, insulin was incubated with continuous shaking (960 rpm) in a Fluoroskan Ascent CF fluorescence plate reader (Labsystems) at 37 °C (excitation at 444 nm, emission at 485 nm) with bottom reading. For the seeding experiments and the effect of urea, TMAO, and sucrose, insulin solutions were incubated in the Fluoroskan Ascent CF fluorescence plate reader at 43 °C without agitation. Insulin adsorption to the plates was investigated by incubating an insulin solution in the plate for 10 min at 37 °C with stirring, and determining the insulin concentration before and after incubation by measuring the UV absorbance. No evidence of insulin adsorption was observed. Three to eight replicates were performed in the plate-reader assays, and the ThT readings for each time point were then averaged.

For fibril formation in glass vials, 10 μL aliquots were withdrawn from the glass vials as described above and added directly to the fluorescence cuvette (1 cm path length semi-micro quartz cuvette) containing 1 mL of a ThT mixture [5 μM ThT, 50 mM Tris buffer, and 100 mM NaCl (pH 7.5)]. Fluorescence measurements were performed using a FluoroMax-2 spectrofluorometer (Instruments S. A., Inc., Jobin Yvon-Spex). The light source was a 150 W xenon lamp. Emission spectra were recorded immediately after addition of the aliquots to the ThT mixture from 470 to 560 nm (excitation at 450 nm, 1 nm increment, 1 s integration time, and slits of 5 nm for both excitation and emission). For each sample, the signal was obtained as the ThT intensity at 482 nm from which was subtracted a blank measurement recorded prior to addition of insulin to the ThT solution. Data were processed using DataMax/GRAMS software.

Circular Dichroism (CD) Spectroscopy. CD spectra were obtained at ambient temperature on an AVIV 60DS circular dichroism spectrophotometer (Aviv Association, Lakewood, NJ) using an insulin concentration of 2 mg/mL. In the near-UV region, CD spectra were recorded in a 1 cm cell from 320 to 250 nm. In the far-UV region, CD spectra were recorded in a 0.01 cm cell from 250 to 190 nm. Both near- and far-UV CD spectra were recorded using a step size of 0.5 nm, a bandwidth of 1.5 nm, and an averaging time of 5 s. For the spectra at ambient temperature, an average of five scans were obtained. For the spectra at 60 °C, only one scan was recorded, and the temperature in the cell was maintained at 60 °C using a circulating water bath. The samples were equilibrated at 60 °C for 10 min before collecting the spectra at 60 °C. CD spectra of the appropriate buffers were recorded and subtracted from the protein spectra. The molar ellipticity, $[\theta]$, was calculated as the CD signal $\times$ molecular mass (in daltons)/[number of residues $\times$ insulin concentration (in milligrams per milliliter) $\times$ cell path length (in millimeters)].

Atomic Force Microscope (AFM) Imaging. A bovine insulin (1 mg/mL) solution in 0.1 M HCl (pH 1.6) was incubated at 37 °C with stirring for 1 h. An aliquot of 5 μL was diluted 10-fold in 0.1 M HCl, and 5 μL of the diluted sample was deposited on freshly cleaved mica and dried immediately with nitrogen gas. The samples were imaged with an Autoprobe CP AFM (Park Scientific, Sunnyvale, CA), in the noncontact mode (NC-AFM). The NC-AFM is an imaging mode in which the cantilever is set vibrating in the z direction at a resonant frequency of $\sim$100 kHz. Approaching the sample results in a dampening of the amplitude of vibration of the cantilever. A tube scanner scans the sample and moves it in the z direction to keep the amplitude of vibration constant. The tube scanner was a 100 μm Scanmaster (Park Scientific), and NC Ultralevers (Park Scientific) were used as cantilevers. The resonant frequency was $\sim$100 kHz. The images were taken in air, under ambient conditions, at a scan frequency of 1$-$2 Hz, using silicon nitride tips.

Small-Angle X-ray Scattering (SAXS). The association state of insulin was determined using a SAXS instrument on beamline 4-2 at Stanford Synchrotron Radiation Laboratory. Insulin (2 mg/mL) was dissolved in 0.025 M HCl and 0.1 M NaCl at pH 1.6, 20 mM formate and 0.1 M NaCl at pH 3.0, 20 mM phospate and 0.1 M NaCl at pH 7.4, and 20% acetic acid and 0.1 M NaCl at pH 1.6. Scattering patterns were recorded by a linear position-sensitive proportional counter, which was filled with an 80% Xe/20% CO_2 gas mixture. Scattering patterns were normalized by incident X-ray intensity, which was measured with a short length ion chamber in front of the sample. The sample-to-detector distance was calibrated to be 230 cm, using a cholesterol myristate sample. To avoid radiation damage of the sample, the protein solution was continuously passed through a 1.3 mm path length observation flow cell with 25 μm mica windows. Background measurements were performed before and after each protein measurement and then averaged before being used for background subtraction. All SAXS measurements were performed at 23 $\pm$ 1 °C.

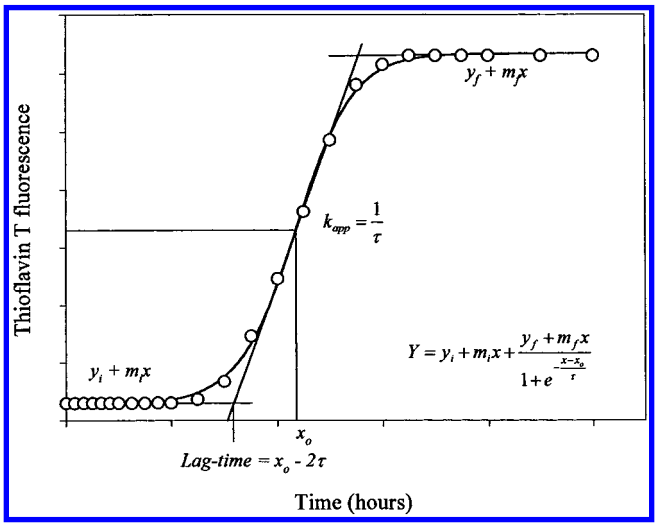

FIGURE 1: Schematic illustration of the sigmoidal increase in thioflavin T fluorescence upon insulin fibril formation. The data were simulated using the M ⇔ I ⇔ nucleus → fibrils scheme and then curve-fit by eq 1. The lag time is approximated by $x_o - 2\tau$, and the apparent rate constant, k_{app}, for fibril growth is given by $1/\tau$ (see Materials and Methods).

The values of the radii of gyration (R_g) were calculated according to the Guinier approximation (*39*):

$$\ln I(Q) = \ln I(0) - R_g^2 Q^2/3$$

where Q is the scattering vector given by $Q = (4\pi \sin \theta)/\lambda$ (2θ is the scattering angle, and λ is the X-ray wavelength). The value of $I(0)$, the forward scattering amplitude $I(Q)$ as $Q \rightarrow 0$, is proportional to the square of the molecular mass of the molecule (*39*). $I(0)$ for a pure dimer sample will therefore be twice that for a sample with the same number of monomers since each dimer will scatter four times as strongly, but there will be half as many as in the pure monomer sample.

Data Evaluation of Kinetics of Fibril Formation. The kinetics of insulin fibril formation could be described as sigmoidal curves defined by an initial lag phase, where no change in ThT fluorescence intensity was observed, a subsequent growth phase in which ThT fluorescence increased, and a final equilibrium phase, where ThT fluorescence reached a plateau indicating the end of fibril formation (Figure 1). Analysis of the data showed that it was consistent with the following kinetic scheme:

$$\text{M} \Leftrightarrow \text{I} \Leftrightarrow \text{nucleus} \rightarrow \text{fibrils}$$

where M is the monomer and I is the intermediate. The kinetic scheme, when simulated, gives sigmoidal curves such as that in Figure 1. For simplicity in comparing effects of different incubation conditions on fibrillation kinetics, the ThT fluorescence measurements were plotted as a function of time and fitted by a sigmoidal curve described by the following equation using SigmaPlot

$$Y = y_i + m_i x + \frac{y_f + m_f x}{1 + e^{-[(x - x_o)/\tau]}} \quad (1)$$

where Y is the fluorescence intensity, x is time, and x_o is the time to 50% of maximal fluorescence. Thus, the apparent rate constant, k_{app}, for the growth of fibrils is given by $1/\tau$, and the lag time is given by $x_o - 2\tau$.

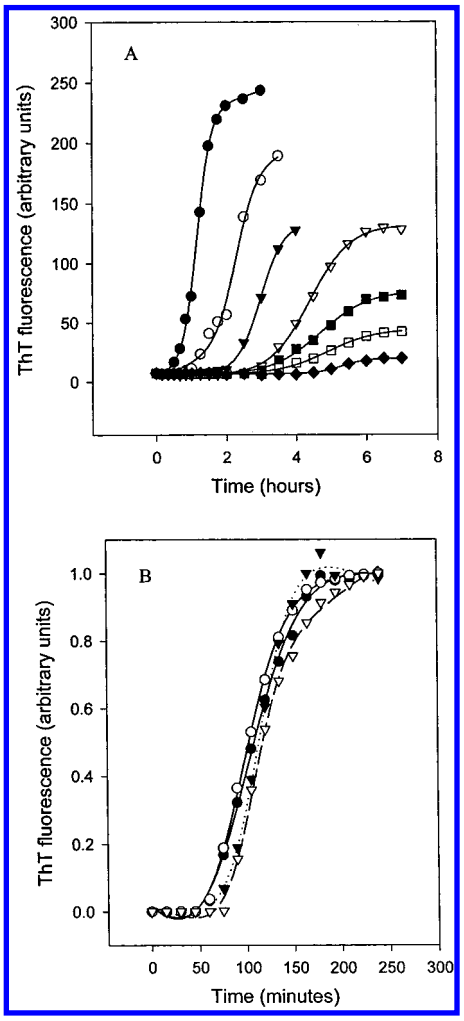

FIGURE 2: Influence of insulin concentration on insulin fibril formation monitored by ThT fluorescence: (A) 60 °C without agitation and (B) 37 °C with vigorous agitation (960 rpm). The symbols represent ThT fluorescence intensities determined experimentally, and the lines are fitted sigmoidal curves according to eq 1. (A) Insulin concentrations were 20 (●), 10 (○), 5 (▼), 2 (▽), 1 (■), 0.5 (□), and 0.2 mg/mL (◆) in 0.025 M HCl and 0.1 M NaCl (pH 1.6). Calculated lag times and rate constants are shown in Table 1. (B) Insulin concentrations were 5 (▽), 1 (▼), 0.05 (○), and 0.01 mg/mL (●) in 0.025 M HCl and 0.1 M NaCl (pH 1.6). The fluorescence intensities were normalized on a scale from 0 to 1.

RESULTS

Effects of Agitation on Insulin Fibrillation Kinetics. At 37 °C, no fibrils were formed under standard conditions (2 mg/mL insulin) in the ThT plate-reader assay at either neutral or acidic pH after 20 h in the absence of agitation (shaking), whereas with agitation, fibrils were formed within 2 h at acidic pH (data not shown). Comparison of the kinetics of fibrillation as a function of the level of agitation in the ThT plate-reader assay indicated that vigorous agitation had a dominant effect on the kinetics of aggregation. For example, when the effect of insulin concentration on fibrillation kinetics was monitored with vigorous shaking (960 rpm), negligible differences in the kinetics were observed as a function of concentration, in contrast to the case when the samples were not shaken (see Figure 2). Similarly, the effects of variations in ionic strength with vigorous shaking were

Table 1: Lag Time and Growth Rate Constants for Insulin Fibril Formation Depend on Insulin Concentration[a]

insulin concentration (mg/mL)	lag time (h)	k_{app} (h^{-1})
0.2	4.6	2.8
0.5	3.5	1.5
1.0	3.3	1.5
2.0	3.3	1.7
5.0	2.3	2.9
10.0	1.7	3.4
20.0	0.8	4.9

[a] Fibril formation at 60 °C without agitation was monitored by in situ ThT fluorescence using 20 μM ThT in 0.025 M HCl and 0.1 M NaCl (pH 1.6). Typical errors (standard deviation) were 19% on the lag times and 27% on the rate constants. Lag times and rate constants were determined using eq 1.

Table 2: pH Dependence of Insulin Fibril Formation[a]

pH	medium	ionic strength (calcd)	lag time (h)	k_{app} (h^{-1})
1.6	25 mM HCl and 0.1 M NaCl	0.12	0.9	6.4
3.0	20 mM formate and 0.1 M NaCl	0.12	1.6	5.7
7.4	20 mM phosphate and 0.1 M NaCl	0.12	13.2	0.6

[a] Fibril formation in glass vials at 37 °C with stirring was monitored by the thioflavin T assay. The insulin concentration was 1 mg/mL. Typical errors (standard deviation) were 25% on the lag times and 32% on the rate constants. Lag times and rate constants were determined using eq 1.

Table 3: Effect of Anions and Ionic Strength on Lag Time and Growth Rate Constant for Insulin Fibrillation[a]

	lag time (h)		k_{app} (h^{-1})	
ionic strength (M)	60 °C without agitation	37 °C with agitation	60 °C without agitation	37 °C with agitation
NaCl				
0.05	3.3	1.6	3.5	0.12
0.10	2.9	1.4	2.4	0.14
0.20	2.6	1.3	1.3	0.11
0.50	2.1	1.5	0.8	0.05
Na_2SO_4				
0.05	3.5	2.0	2.4	0.08
0.10	3.0	2.2	3.2	0.05
0.20	3.6	1.5	1.3	0.05
0.50	11.5	1.4	0.8	0.04
NaH_2PO_4				
0.05	3.5	1.5	0.5	0.12
0.1	2.0	1.6	0.6	0.11
0.2	1.9	1.6	0.6	0.08
0.5	1.1	1.6	0.8	0.06

[a] Fibril formation was monitored by in situ ThT fluorescence at 60 °C without agitation and at 37 °C with agitation (960 rpm). The insulin concentration was 2 mg/mL, dissolved in 0.025 M HCl (pH 1.6). The ThT concentration was 20 μM. Typical errors (standard deviation) were 11% on the lag times and 15% on the rate constants. Lag times and rate constants were determined using eq 1.

dramatically attenuated compared to the situation with no shaking (Table 3). Consequently, a number of experiments were performed at both 37 °C with agitation and 60 °C without agitation (at 60 °C, the rate of fibril formation in the absence of shaking or stirring was suitably rapid for convenient analysis).

Effect of Insulin Concentration on Fibril Formation. When insulin solutions were incubated under conditions leading to fibrils, the fluorescence of ThT at 482 nm followed a characteristic sigmoidal curve, i.e., an initial lag phase, a subsequent growth phase, and a final equilibrium phase, as seen in Figure 2. This curve is consistent with a nucleation-dependent elongation model, in which the three phases (lag, exponential increase, and final leveling off) correspond to nucleation, extension, and equilibrium phases (*11*, *12*, *15*, *40*).

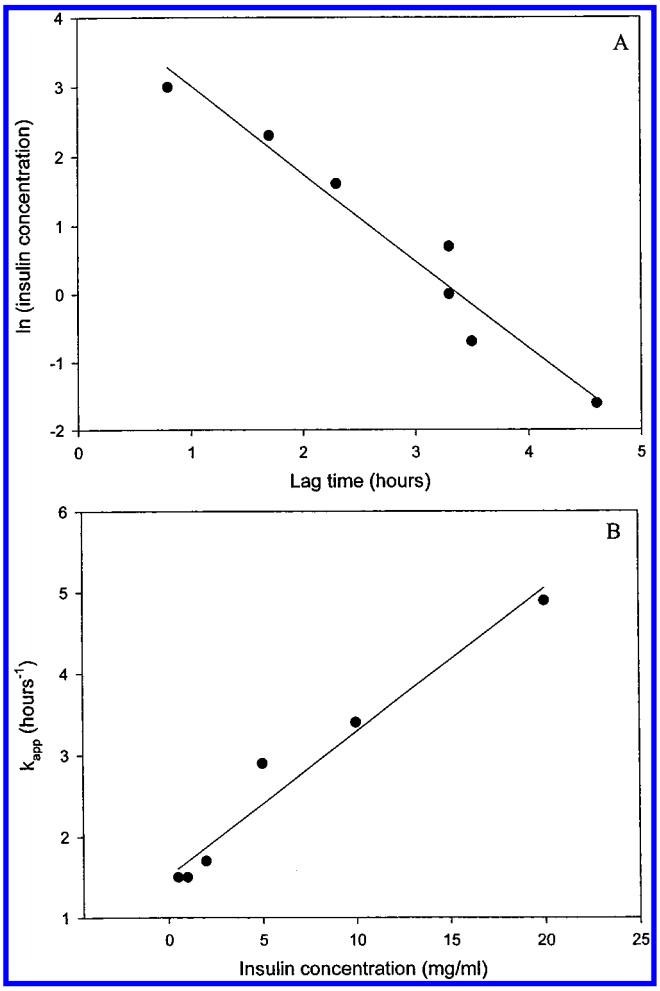

FIGURE 3: Effects of insulin concentration on the kinetics of fibrillation. (A) Inverse linear dependency of the logarithm to insulin concentration as a function of lag time. Fibril formation of insulin at 60 °C, no agitation, in 0.025 M HCl and 0.1 M NaCl (pH 1.6). (B) Linear dependency of the apparent rate constant, k_{app}, for fibril growth on the insulin concentration.

The influence of insulin concentration on the kinetics of fibril formation at 60 °C, without agitation, is illustrated in Figure 2A. The sigmoidal curves were fitted according to eq 1. The lag times and the apparent first-order rate constants for fibril growth were determined from the curve fits and are shown in Table 1. An increase in the insulin concentration resulted in a decrease in the lag time and an increase in the apparent rate constants for fibril growth (Table 1). There was an inverse linear correlation between the logarithm of insulin concentration and the duration of lag time (Figure 3A). The rate of elongation of fibrils is consistent with a first-order reaction, based on the good fit of the data to eq 1. There was also a linear dependency of the apparent first-order rate constant for fibril growth on insulin concentration (Figure 3B).

The physical appearance of the fibrillated insulin solutions depended on the initial insulin concentration. For concentrations of ≥5 mg/mL, the end state of the fibrillated insulin

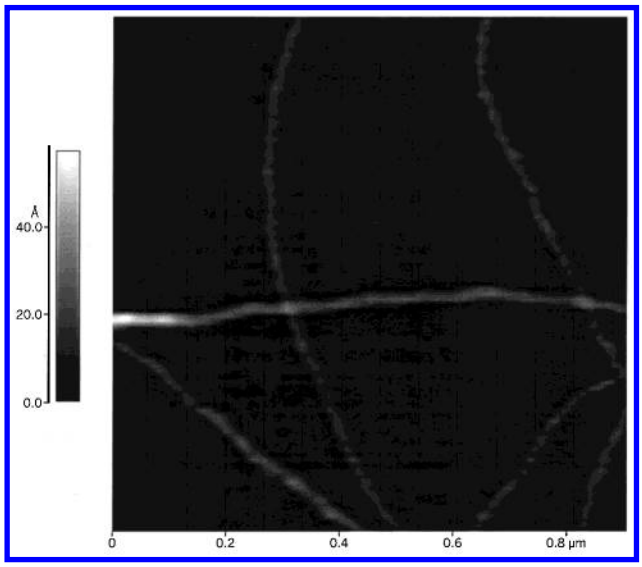

FIGURE 4: Atomic force microscope (AFM) images of insulin fibrils grown in HCl (pH 1.6). Note the braided structure. The scale bar on the left represents the height of the sample; the lighter the color, the higher the sample is from the surface. The average height of the fibrils was 21 Å, corresponding to an average diameter of 21 Å.

solutions consisted of a firm, turbid gel. At concentrations of ≤2 mg/mL, the fibrillated state was a viscous solution containing visible aggregates. A similar dependency of the appearance of the fibrillated solutions on the concentration has been observed for human calcitonin fibrils (*41*). As an insulin concentration of 2 mg/mL gave a reasonable lag time for fibril formation and a reasonable increase in ThT fluorescence upon fibril formation, this concentration was used for further studies. A typical atomic force microscope (AFM) image of insulin fibrils from relatively early in the fibril growth phase is shown in Figure 4 (at later times, the fibrils were much more clumped together; data not shown). The fibrils averaged 21 ± 3 Å in height, corresponding to an average diameter of 21 Å, and showed evidence of braiding.

Effect of pH on Insulin Fibril Formation. Prior to investigating the effect of pH on insulin fibrillation, we studied the conformation of insulin as a function of pH. The far-UV CD spectra of insulin measured at different pH values (pH 1.6−7.5) were very similar (Figure 5A). This means that there is no evidence for significant distortion of the insulin secondary structure induced by the decrease in pH. However, the near-UV CD spectra of insulin revealed some loss of tertiary structure under conditions of low pH (pH ≤3) (Figure 5B). It is known that dissociation of insulin oligomers into monomers is reflected by a weakening of the negative band at 275 nm arising from the tyrosines (B16 and B26) in the monomer−monomer interface (*42*, *43*). At 60 °C, insulin shows some loss in the far-UV CD signal and a substantial decrease in the magnitude of the near-UV CD signal (Figure 5). However, it is evident from Figure 5 that insulin still retains substantial secondary and tertiary structure even under conditions of extremely low pH or at elevated temperatures. SAXS analysis shows that insulin is hexameric at pH 7.4 (R_g = 19.8 Å), tetrameric at pH 3.0 (R_g = 17.8 Å), dimeric at pH 1.6 (R_g = 14.9 Å), and monomeric in 20% acetic acid at pH 1.6 (R_g = 11.6 Å).

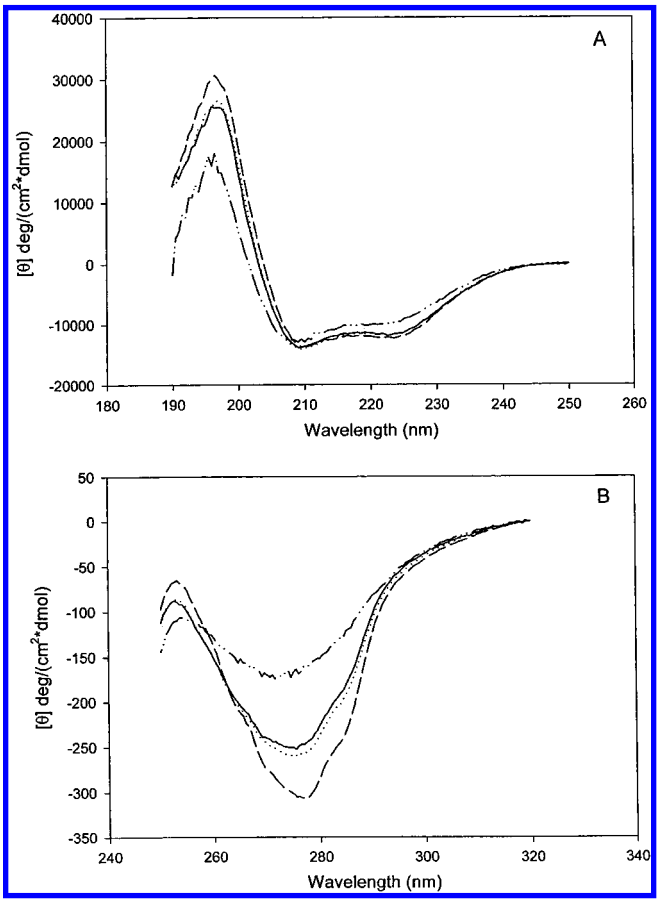

FIGURE 5: Far-UV (A) and near-UV CD spectra (B) of insulin (1 mg/mL) measured at ambient temperature in 0.025 M HCl and 0.1 M NaCl at pH 1.6 (—), 20 mM formate and 0.1 M NaCl at pH 3.0 (••••), and 20 mM phosphate and 0.1 M NaCl at pH 7.4 (− − −). The CD spectra of insulin measured at 60 °C in 0.025 M HCl and 0.1 M NaCl at pH 1.6 (−••−) are shown for comparison. See Materials and Methods for details.

The effect of pH on fibril formation at 37 °C in glass vials with stirring was investigated at three different pH values. Shorter lag times and faster growth of fibrils were seen at acidic pH compared to those measured at neutral pH (Table 2). An increase in pH from 1.6 to 3.0 resulted in a 2-fold increase in lag time and a minor reduction in the growth rate. At neutral pH, the lag time was 15 times longer than at pH 1.6, and the growth rate was reduced almost 12-fold (Table 2). However, when fibril formation was studied in the 96-well plate at 60 °C without stirring at pH 3 and 7.4, no fibrils were formed within 24 h. Thus, a pH of 1.6 was chosen for further studies in the 96-well plate-reader assay, as fibrils were formed at this pH on a convenient time scale.

Effect of Ionic Strength and Acid Media on Insulin Fibril Formation. The influence of ionic strength on insulin fibrillation was studied at pH 1.6 with and without agitation. Comparing the complete kinetic curves (data not shown) for fibril formation as a function of anion, in the absence of agitation, indicated that at low ionic strength the order was sulfate ∼ chloride > phosphate, whereas at high ionic strength, the order was chloride > phosphate > sulfate. In the presence of vigorous agitation, there were no significant differences in the overall rates of fibrillation. The calculated lag times and apparent rate constants for fibrillation of insulin in the presence of increasing concentrations of sodium chloride, sodium sulfate, and sodium dihydrogen phosphate

Table 4: Lag Time and Apparent Growth Rate Constant for Insulin Fibril Formation as a Function of Acid (HCl, H_2SO_4, and H_3PO_4) Concentrations[a]

medium concentration (M)	lag time (h)	k_{app} (h^{-1})	pH	ionic strength (calcd)
HCl				
0.025	9.4	0.6	1.7	0.025
0.05	7.7	1.9	1.4	0.05
0.10	3.8	3.8	1.1	0.1
0.20	3.6	1.1	0.9	0.2
0.50	2.3	0.8	0.5	0.5
H_2SO_4				
0.017	11.7	1.5	1.7	0.036
0.033	9.8	1.1	1.5	0.063
0.05	10.6	0.8	1.3	0.088
0.067	9.5	0.7	1.2	0.11
0.10	6.7	0.6	1.1	0.16
0.20	3.2	0.7	0.9	0.29
0.50	2.6	1.5	0.5	0.64
H_3PO_4				
0.1	14.2	0.5	1.6	0.024
0.2	12.5	0.4	1.4	0.035
0.5	7.6	1.3	1.2	0.058

[a] Fibril formation at 60 °C without agitation was monitored by in situ ThT fluorescence using 20 μM ThT. The insulin concentration was 2 mg/mL. Typical errors (standard deviation) were 20% on the lag times and 28% on the rate constants. Lag times and rate constants were determined using eq 1.

are shown in Table 3. With the exception of sulfate, increased ionic strength led to shorter lag times. In the samples that were agitated, the effects were attenuated, compared to those incubated in the absence of agitation. There was no clear correlation between the rate constant k_{app} for fibril growth and ionic strength. In general, an increase in ionic strength resulted in slower growth of the fibrils, with the exception of phosphate, in the absence of agitation. The effects of increasing concentration of the acids, hydrochloric acid, sulfuric acid, and phosphoric acid, were also examined. The calculated lag times and apparent rate constants for fibrillation are shown in Table 4. For each acid, increased concentrations led to shorter lag times However, no direct correlation between the concentration of the acids and the rate of fibril growth was observed.

Effect of ANS and ThT on Insulin Fibril Formation. The hydrophobic fluorescent dye, ANS, is known to bind preferentially to partially folded intermediates (*44*), and is thus a good probe for the presence of such species. When ANS was present in the insulin incubation solutions, the ANS was observed to inhibit fibril formation. A 10-fold molar excess of ANS resulted in a 3-fold increase in the length of the lag time and a 3-fold reduction in the growth rate. With a 50-fold molar excess of ANS, no insulin fibrils were formed within 24 h. In both cases, addition of ANS to the insulin solutions resulted in immediate protein precipitation. In contrast to ANS, ThT did not affect the kinetics of insulin fibril formation significantly (data not shown). The calculated lag times and apparent rate constants for insulin fibril formation with and without ThT were identical within experimental error.

Effect of the Denaturant and Stabilizers on Insulin Fibril Formation. The denaturant, urea, had an accelerating effect on insulin fibril formation at pH 7.4 (Table 5). When insulin was incubated at 43 °C without agitation, no fibrils were formed under neutral conditions within 48 h. Addition of increasing concentrations of urea to insulin at pH 7.4 resulted in decreasing lag times and slightly increasing elongation rate constants (Table 5). The effect of the stabilizers, TMAO and sucrose, was investigated under monomeric conditions, i.e., in acetic acid. The presence of both TMAO and sucrose resulted in longer lag times at pH 1.6 (Table 5), indicating a stabilizing effect on the native insulin conformation.

Table 5: Influence of Urea, TMAO, and Sucrose on the Kinetics of Insulin Fibril Formation[a]

	lag time (h)	k_{app} (h^{-1})	pH
denaturant			
control	>48	nd[b]	7.5
2 M urea	17.3	0.15	7.4
4 M urea	8.1	0.29	7.4
6 M urea	2.8	0.39	7.4
stabilizer			
control	2.96	0.87	1.6
1 M TMAO	7.05	3.11	1.6
10% sucrose	5.62	1.10	1.6

[a] Fibril formation was monitored by in situ ThT fluorescence at 43 °C without agitation. The ThT concentration was 20 μM. The insulin concentration was 2 mg/mL dissolved in either 20 mM phosphate and 0.1 M NaCl (pH 7.4) or 20% acetic acid and 0.1 M NaCl (pH 1.6). Typical errors (standard deviation) were 18% on the lag times and 26% on the rate constants. Lag times and rate constants were determined using eq 1. [b] Not determined.

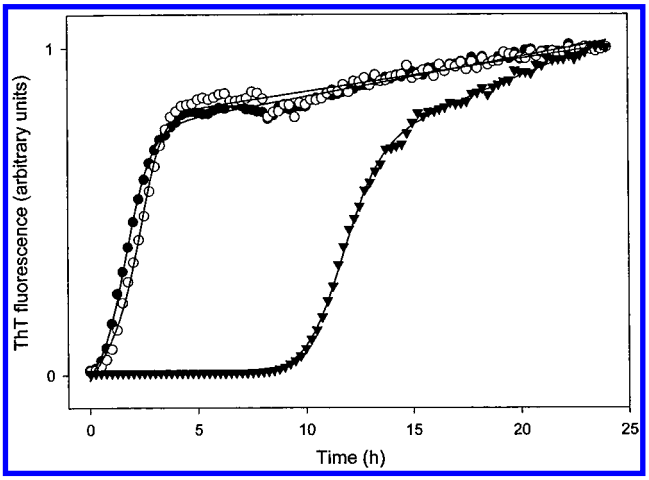

FIGURE 6: Influence of seeding on insulin fibril formation at 43 °C monitored by ThT fluorescence. The symbols represent ThT fluorescence intensities determined experimentally, and the lines are fitted according to eq 1. Insulin (2 mg/mL) in 0.025 M HCl and 0.1 M NaCl at pH 1.6 (▼), 0.05% fibril seeds added (○), and 0.1% fibril seeds added (●). The fluorescence intensities were normalized on a scale from 0 to 1.

Effect of Seeding on Insulin Fibril Formation. When insulin was incubated in HCl at pH 1.6 and 43 °C without agitation, the lag time of fibril formation was 9.3 h and the elongation rate constant was 0.77 h^{-1} (Figure 6). The addition of 0.5% fibril seeds to a fresh solution resulted in a 10-fold decrease in the lag time and a 2-fold increase in the rate of elongation. Addition of fibril seeds at concentrations of 1, 5, and 10% relative to the concentration of the native insulin completely eliminated the lag phase.

DISCUSSION

Exposure of proteins to acidic pH and high temperatures for prolonged periods of time may result in significant

chemical degradation. The main degradation reaction of insulin under acidic conditions is deamidation at Asn^{A21} (*45*). Even though some deamidation is expected under the acidic conditions used in these experiments, it is considered to be of minor importance, since the deamidated form of insulin has the same fibrillation properties and structural properties as the native insulin (*36*). According to the European Pharmacopoeia, some deamidation of insulin is allowed in insulin preparations for human use (not more than 5% A12 desamidoinsulin). As noted, a low pH is used in the manufacture of insulin for use by diabetics.

The characteristic sigmoidal curve of ThT fluorescence, seen when insulin fibrils are formed, is also seen for amyloid β-peptide aggregation (*46*, *47*) and most other amyloid systems. The kinetics of insulin fibril formation were characterized by two independent factors that determined the overall rate of fibril formation: lag time (related to how fast the nuclei are formed) and fibril growth (the rate of fibril elongation). Previous studies suggest that the minimum kinetic scheme for formation of insulin fibrils involves the following major steps (manuscript submitted for publication):

$$\text{hexamer/tetramer/dimer} \rightarrow \text{monomer} \rightarrow \text{intermediate} \rightarrow \text{nucleus} \rightarrow \text{filament/fibril}$$

Thus, for fibril formation to occur, the hexameric or tetrameric associated states of insulin at neutral pH, or the dimers at low pH, must initially dissociate into monomeric molecules, which are in equilibrium with a partially folded conformation (manuscript submitted for publication; *17*) that undergoes oligomerization to form the critical nucleus. This step is assumed to involve a number of additional intermediates (soluble oligomers) for which the equilibrium disfavors the nucleus, accounting for the lag phase observed in the kinetics of fibrillation.

Nucleation Process. Although the sigmoidal curve fits for the ThT kinetic data gave very good fits, the expression given in eq 1 must be considered an empirical approximation of the real underlying kinetic scheme, especially with respect to the lag time. However, as noted, simulation of the underlying kinetics scheme gave curves that were very well fit by eq 1. We assume that the lag time is directly related to the length of time it takes to form the nucleus. This is supported by the fact that addition of seeds essentially eliminated the lag phase. The seeding effect is characteristic of a nucleation-dependent elongation mechanism (*12*). The observed inverse linear correlation between the log of the insulin concentration and the lag time must reflect some aspect of the underlying kinetics associated with formation of the nucleus. As discussed subsequently, we believe that the rate-limiting step in insulin nucleation is the formation of the aggregation-competent intermediate, which would be expected to be a first-order process. If this is correct, the influence of ionic strength and anions on nucleation (i.e., lag time) is likely to have an effect on the conformational stability of the intermediate or on the rate of formation of the intermediate. This hypothesis involves a model in which the key partially folded intermediate conformation, once formed, oligomerizes very rapidly to form insoluble fibrils. Supporting evidence for this is the effect of vigorous agitation and the effects of denaturant and stabilizers, as discussed below.

The decrease in the lag time of fibril formation with increasing ionic strength can be explained by the shielding of repulsive charges between the interacting insulin molecules, and thereby a promotion of fibril formation. At pH 1.6, the insulin monomer has a net positive charge of 6 (*26*). Addition of the chloride, sulfate, and phosphate anions will thus screen these positive charges and make hydrophobic interactions, which are necessary for self-association and formation of nuclei, more favorable (*48*). Thus, the results indicate that nucleation of insulin is controlled by both electrostatic and hydrophobic interactions. For human calcitonin, it has been proposed that electrostatic interactions between calcitonin monomers play an important role in the initial aggregation step (*41*). Electrostatic interactions were also important for glycosaminoglycan-induced fibrillation of amyloid-β peptide 1−40 (Aβ40) (*49*). There are also data to indicate that both electrostatic and hydrophobic interactions were involved in fibril formation of amyloid-β peptide (*50*).

The lack of linear dependency of lag time on ionic strength (Table 3) indicates that ionic strength is not the only factor that influences the lag time of insulin fibril formation. It is observed that HCl and NaCl at low concentrations, 0.05 M, have different lag times (7.7 and 3.3 h, respectively; Tables 3 and 4). Since the anions are the same in both cases, the difference may be explained in terms of the cations, H^+ and Na^+, as cations have been seen to influence aggregation of proteins (*51*, *52*). At concentrations of <0.5 M, NaCl is more effective in promoting fibril formation than HCl. It would therefore appear that cations may also be involved in the formation of the critical nucleus. Further studies investigating the influence of monovalent and divalent cations on insulin fibril formation are in progress.

Fibril Elongation. The rate of elongation of fibrils is also consistent with a first-order reaction, based on the good fit of the data to eq 1; the term in the denominator of eq 1 corresponds to the exponential growth part of the sigmoidal curve, i.e., the latter half of the sigmoid. The kinetics of elongation have been shown to follow first-order kinetics for other proteins, including α-synuclein and amyloid β-protein (*13*, *15*, *46*, *53*). The simplest explanation for the linear dependency of the apparent first-order rate constant for fibril growth on insulin concentration is that increasing the concentration of insulin leads to increasing numbers of fibrils, due to the increasing concentration of nuclei.

Fibril formation was slower in phosphoric acid than in hydrochloric acid or sulfuric acid. This can be explained by the fact that H_3PO_4 is a much weaker acid than both HCl and H_2SO_4. The smaller degree of dissociation of phosphoric acid provides smaller amounts of negatively charged anions that would be able to screen the repulsive positive charges between the interacting insulin molecules. Consequently, the formation of a nucleus is not favored, and fibril formation proceeds more slowly in phosphoric acid.

There is no clear-cut correlation between the rate of fibril elongation and ionic strength or acid concentration as seen in Tables 3 and 4. However, the generally slower rates of elongation at higher ionic strength or increasing acid concentration indicate that increasing the concentration of anions slows the fibril elongation process. This could reflect the role of electrostatics in elongation, and that at elevated anion concentrations the electrostatic attraction between fibril

and monomer or partially folded intermediate (or soluble oligomer) is screened by the ions.

Agitation Effects. The fact that vigorous agitation attenuated the effects of insulin concentration or ionic strength indicates that agitation is a particularly critical factor in insulin fibrillation. Previous investigations have demonstrated the important role of hydrophobic surfaces in insulin aggregation, in particular air−water and Teflon−water interfaces (*18*). Thus, the enhanced rates of fibrillation with strong agitation undoubtedly arise from the increased amount of air−water interface. Interestingly, the addition of a small Teflon bead to the agitated (960 rpm) insulin incubation solution had no significant effect on the kinetics of fibrillation in the studies presented here, indicating that the small additional hydrophobic interface was negligible to that caused by the strong agitation. It should be noted that the shaking rate used in the 37 °C plate-reader assays (960 rpm) is much higher than that of 80−250 rpm used previously (*18*).

The most reasonable explanation for the role of the air−water interface in fibrillation is that it promotes the (partial) denaturation of the protein. This leads to the buildup of a partially folded intermediate that is a critical species on the fibrillation pathway. Furthermore, the essentially identical fibrillation kinetics observed with strong agitation, regardless of the insulin concentration, in comparison to the marked concentration effects in the absence of agitation, indicate that the rate-limiting step in the absence of agitation is formation of the fibrillation-competent intermediate. At low pH, the net positive charge on insulin will make it more sensitive to denaturation; the additional destabilization brought about by the air−water interface when samples are incubated with agitation will lead to a shift in the equilibrium from the native state (N) to the partially folded intermediate (I) and the unfolded state (U), as in the following scheme:

$$N \leftrightarrows I \leftrightarrows U$$

It is well-known that the addition of salts (more specifically, anions) to proteins that are unfolded at low pH leads to their becoming more compact and adopting a partially folded intermediate conformation (*54*). Thus, increasing ionic strength, under conditions of low pH and vigorous agitation, would be expected to significantly populate the partially folded intermediate (rather than the unfolded state). We also attribute the observed decrease in lag time with increasing concentration of acid to this phenomenon; the increasingly lower pH values may potentially increase the concentration of U, but the corresponding increase in anion concentration will have a more significant effect in increasing the concentration of the intermediate, I.

At 37 °C, there was no significant effect of insulin concentration on the rate of fibrillation when agitated at low pH, whereas when it is agitated at neutral pH, lower concentrations lead to faster fibrillation (*18*), presumably because the lower protein concentration increases the amount of monomer. In the absence of agitation at neutral pH, fibrils form very slowly, indicating that agitation is necessary for the intermediate to build up.

As expected, shorter lag times of insulin fibril formation were observed in the presence of the denaturant, urea, and longer lag times in the presence of the stabilizers, TMAO and sucrose, indicating the importance of the buildup of the partially folded intermediate during the lag phase. The most reasonable explanation is that urea, by destabilizing the conformation of insulin, promotes the population of the partially folded intermediate, which will lead to a decrease in the lag time. In contrast, TMAO and sucrose have a stabilizing effect, and therefore shift the equilibrium to the native state and away from the partially folded intermediate, resulting in longer lag times. The dramatic effect of seeding on the lag times also supports the importance of a partially folded intermediate.

During the first 10 min at 60 °C, the secondary structure of insulin was only slightly altered, whereas the tertiary structure was significantly changed. This is most likely due to the presence of a partially folded intermediate with relatively native-like secondary structure. On the basis of the near-UV CD signal observed at 60 °C, compared to that of native and fully unfolded insulin, we estimate that the putative intermediate has approximately 53% of the native tertiary structure. Partially folded intermediates typically have relatively native-like secondary structure, but relatively little near-UV CD signal. Upon further incubation at 60 °C, the far-UV CD spectra of insulin exhibited a significant loss of the signal, due to either conformational changes and/or loss of protein material due to fibril formation (data not shown).

Effect of ANS on Insulin Fibrillation. Under conditions of low protein and ANS concentrations, there was evidence that ANS binds to insulin, as an increase in ANS fluorescence intensity and a blue shift in emission maximum were observed (data not shown). This is further confirmation of the existence of a partially folded intermediate. However, upon addition of high ANS concentrations to the concentrated insulin solutions, protein precipitation was observed. The most plausible explanation for this phenomenon is that ANS binds to the intermediate, and at higher concentrations causes insulin to form amorphous aggregates as an alternative pathway to fibril formation. Since the precipitate is not fibrillar, we assume it is amorphous in nature. Since the precipitation will cause depletion of native insulin molecules from the solution, the increase in lag time and reduction in the growth rate upon addition of ANS can therefore be interpreted to be due to a decrease in insulin concentration. The results also indicate that the conversion of amorphous precipitates into fibrils is either very slow or nonexistent. Another possibility is that ANS binds to insulin at low pH due to electrostatic interactions. Insulin has a net positive charge of 6 at pH 1.6, while the sulfonate group of ANS is negatively charged. This would explain the interaction of ANS with insulin at low pH. The precipitation observed could simply be a precipitation of an insulin−ANS complex. The very different effects observed when ANS or ThT was present indicate that these two dyes must have quite different modes of interaction with insulin during fibrillation. The data are most consistent with ThT only interacting significantly with fibrils, rather than intermediates on the pathway to fibrils.

Model for Insulin Fibrillation. We propose that the early stages of insulin fibril formation involve the dissociation of native associated states (hexamer, tetramer, and dimer) to give native monomer, which is in equilibrium with the fibrillation-competent partially folded intermediate. This intermediate then oligomerizes to form transient soluble oligomers that lead to the nucleus. In the absence of vigorous

Scheme 1: Model for Insulin Fibrillation[a]

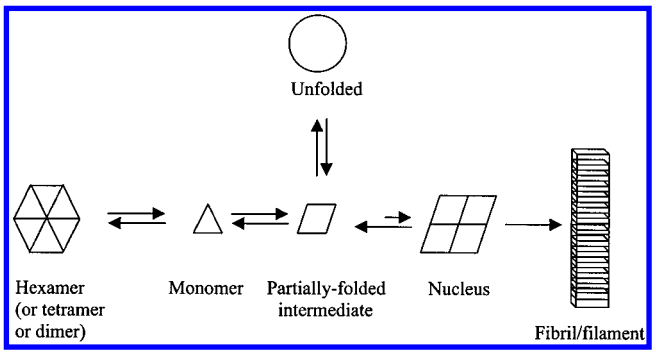

[a] Different shapes represent different conformations. The nucleus is shown schematically and probably consists of a large number of subunits.

agitation, the equilibrium will favor the associated native states; however, in the presence of significant interfacial interactions, the equilibrium will shift in favor of the intermediate. Once formed, the intermediate, which must have a strong propensity to oligomerize, will inevitably lead to fibrils above some critical threshold concentration (Scheme 1). The partially folded intermediate is likely to resemble the relatively unfolded intermediate observed by Millican and Brems (*17*).

Support for the existence of a critical partially folded intermediate conformation on the fibrillation pathway for insulin comes from the ANS binding, the effect of agitation, and the near-UV CD spectra. Although the spectral changes in the near-UV CD spectra could be due to pH-induced dissociation of insulin, as insulin is less associated at lower pH values than at neutral pH (*55*), it is possible that it results from a conformational change associated with formation of the intermediate; that is, a tertiary conformational change at low pH both triggers the dissociation and leads to the intermediate. The fact that fibril formation occurred relatively rapidly at 60 °C in the absence of agitation, compared to 37 °C where fibrillation was not observed, is also consistent with the critical intermediacy of a partially folded intermediate. The higher temperature will favor a shift in the equilibrium between native associated forms of insulin to an increased population of the partially folded intermediate, which is also consistent with the CD spectra at 60 °C. Our observations are consistent with a kinetic scheme in which the formation of the fibrillation-competent intermediate is the rate-limiting step under most conditions, a possible exception being conditions of vigorous agitation, in which the agitation leads to such a large air−water interfacial area that the concentration of the intermediate is very rapidly built up.

It is important to note that factors influencing the nucleation and elongation do not necessarily work in the same direction. For example, increasing concentrations of sodium chloride (increasing ionic strength) resulted in faster nucleation, but slower elongation of fibrils. Thus, factors that have an influence on the lag time, or on the rate of fibril growth, will both be potentially of crucial importance to the overall kinetics of fibril formation. The results demonstrate the importance of studying the kinetics of fibril formation in more detail, and identifying the effects of various factors on the different phases of the process. In the search for stabilizing additives for protein pharmaceuticals, for example, it will be important to evaluate their effect on both the nucleation and elongation during fibril formation.

Conclusions. The kinetics of insulin fibrillation were successfully monitored by the fluorescent probe, thioflavin T, and shown to be consistent with a nucleation-dependent elongation mechanism via the initial formation of a partially folded intermediate conformation. The results indicate that both nucleation and fibril growth are controlled by electrostatic and hydrophobic interactions, and that agitation is the most sensitive of the various variables examined in insulin fibrillation.

ACKNOWLEDGMENT

We thank Cristian Ionescu-Zanetti and Sue Carter for assistance with the AFM experiments and Keith Oberg for useful discussions.

REFERENCES

1. Manning, P. K., and Borchardt, R. T. (1989) *Pharm. Res. 6*, 903−918.
2. Fink, A. L. (1998) *Folding Des. 3*, R9−R23.
3. Uversky, V. N., Talapatra, A., Gillespie, J. R., and Fink, A. L. (1999) *Med. Sci. Monit. 5*, 1001−1012.
4. Uversky, V. N., Talapatra, A., Gillespie, J. R., and Fink, A. L. (1999) *Med. Sci. Monit. 5*, 1238−1254.
5. Bryant, C., Spencer, D. B., Miller, A., Bakaysa, D. L., McCune, K. S., Maple, S. R., Pekar, A. H., and Brems, D. N. (1993) *Biochemistry 32*, 8075−8082.
6. Weiss, M. A., Nguyen, D. T., Khait, I., Inouye, K., Frank, B. H., Beckage, M., O'Shea, E., Shoelson, S. E., Karplus, M., and Neuringer, L. J. (1989) *Biochemistry 28*, 9855−9873.
7. Hua, Q. X., and Weiss, M. A. (1991) *Biochemistry 30*, 5505−5515.
8. Brange, J., Andersen, L., Laursen, E. D., Meyn, G., and Rasmussen, E. (1997) *J. Pharm. Sci. 86*, 517−525.
9. Waugh, D. F. (1946) *J. Am. Chem. Soc. 68*, 247−250.
10. Waugh, D. F., Wilhelmson, D. F., Commerford, S. L., and Sackler, M. L. (1953) *J. Am. Chem. Soc. 75*, 2592−2600.
11. Jarrett, J. T., and Lansbury, P. T. (1992) *Biochemistry 31*, 12345−12352.
12. Jarrett, J. T., and Lansbury, P. T. (1993) *Cell 73*, 1055−1058.
13. Lomakin, A., Chung, D. S., Benedek, G. B., Kirschner, D. A., and Teplow, D. B. (1996) *Proc. Natl. Acad. Sci. U.S.A. 93*, 1125−1129.
14. Teplow, D. B. (1998) *Amyloid 5*, 121−142.
15. Wood, S. J., Wypych, J., Steavenson, S., Louis, J. C., Citron, M., and Biere, A. L. (1999) *J. Biol. Chem. 274*, 19509−19512.
16. Brange, J., Dodson, G. G., Edwards, D. J., Holden, P. H., and Whittingham, J. L. (1997) *Proteins 27*, 507−516.
17. Millican, R. L., and Brems, D. N. (1994) *Biochemistry 33*, 1116−1124.
18. Sluzky, V., Tamada, J. A., Klibanov, A. M., and Langer, R. (1991) *Proc. Natl. Acad. Sci. U.S.A. 88*, 9377−9381.
19. Sluzky, V., Klibanov, A. M., and Langer, R. (1992) *Biotechnol. Bioeng. 40*, 895−903.
20. Westermark, P., and Wilander, E. (1983) *Diabetologia 24*, 342−346.
21. Westermark, P., Wernstedt, C., Wilander, E., Hayden, D. W., O'Brien, T. D., and Johnson, K. H. (1987) *Proc. Natl. Acad. Sci. U.S.A. 84*, 3881−3885.
22. Rhoades, E., Agarwal, J., and Gafni, A. (2000) *Biochim. Biophys. Acta 1476*, 230−238.
23. Ehrlich, J., and Ratner, I. M. (1961) *Am. J. Pathol. 38*, 49−59.
24. Storkel, S., Schneider, H. M., Muntefering, H., and Kashiwagi, S. (1983) *Lab. Invest. 48*, 108−111.
25. Dische, F. E., Wernstedt, C., Westermark, G. T., Westermark, P., Pepys, M. B., Rennie, J. A., Gilbey, S. G., and Watkins, P. J. (1988) *Diabetologia 31*, 158−161.

26. Brange, J., Skelbaek-Pedersen, B., Langkjaer, L., Damgaard, U., Ege, H., Havelund, S., Heding, L. G., Jorgensen, K. H., Lykkeberg, J., Markussen, J., Pingel, M., and Rasmussen, E. (1987) in *Galenics of insulin. The physicochemical and pharmaceutical aspects of insulin and insulin preparations*, Springer-Verlag, Berlin.
27. Kusumoto, Y., Lomakin, A., Teplow, D. B., and Benedek, G. B. (1998) *Proc. Natl. Acad. Sci. U.S.A. 95*, 12277−12282.
28. Brown, A. M., Tummolo, D. M., Rhodes, K. J., Hofmann, J. R., Jacobsen, J. S., and Sonnenberg-Reines, J. (1997) *J. Neurochem. 69*, 1204−1212.
29. Clodfelter, D. K., Nussbaum, M. A., and Reilly, J. (1999) *J. Pharm. Biomed. Anal. 19*, 763−775.
30. Ma, J., Yee, A., Brewer, H. B., Das, S., and Potter, H. (1994) *Nature 372*, 92−94.
31. Ionescu-Zanetti, C., Khurana, R., Gillespie, J. R., Petrick, J. S., Trabachino, L. C., Minert, L. J., Carter, S. A., and Fink, A. L. (1999) *Proc. Natl. Acad. Sci. U.S.A. 96*, 13175−13179.
32. Naiki, H., Higuchi, K., Matsushima, K., Shimada, A., Chen, W. H., Hosokawa, M., and Takeda, T. (1990) *Lab. Invest. 62*, 768−773.
33. Levine, H. (1993) *Protein Sci. 2*, 404−410.
34. Levine, H. (1995) *Amyloid 2*, 1−6.
35. Levine, H. (1995) *Neurobiol. Aging 16*, 755−764.
36. Nielsen, L., Frokjaer, S., Carpenter, J. F., and Brange, J. (2001) *J. Pharm. Sci. 90*, 29−37.
37. Bouchard, M., Zurdo, J., Nettleton, E. J., Dobson, C., and Robinson, C. V. (2000) *Protein Sci. 9*, 1960−1967.
38. Porter, R. R. (1953) *Biochem. J. 53*, 320−328.
39. Glatter, O., and Kratky, O. (1982) in *Small angle X-ray scattering*, Academic Press, New York.
40. Lomakin, A., Teplow, D. B., Kirschner, D. A., and Benedek, G. B. (1997) *Proc. Natl. Acad. Sci. U.S.A. 94*, 7942−7947.
41. Arvinte, T., Cudd, A., and Drake, A. F. (1993) *J. Biol. Chem. 268*, 6415−6422.
42. Wood, S. P., Blundell, T. L., Wollmer, A., Lazarus, N. R., and Neville, R. W. (1975) *Eur. J. Biochem. 55*, 531−542.
43. Strickland, E. H., and Mercola, D. (1976) *Biochemistry 15*, 3875−3884.
44. Semisotnov, G. V., Rodionova, N. A., Razgulyaev, O. I., Uversky, V. N., Gripas, A. F., and Gilmanshin, R. I. (1991) *Biopolymers 31*, 119−128.
45. Brange, J., and Langkjaer, L. (1992) *Acta Pharm. Nord. 4*, 149−158.
46. Naiki, H., Hasegawa, K., Yamaguchi, I., Nakamura, H., Gejyo, F., and Nakakuki, K. (1998) *Biochemistry 37*, 17882−17889.
47. Naiki, H., and Gejyo, F. (1999) *Methods Enzymol. 309*, 305−318.
48. Goto, Y., Takahashi, N., and Fink, A. L. (1990) *Biochemistry 29*, 3480−3488.
49. McLaurin, J., Franklin, T., Zhang, X. Q., Deng, J. P., and Fraser, P. E. (1999) *Eur. J. Biochem. 266*, 1101−1110.
50. Fraser, P. E., Nguyen, J. T., Surewicz, W. K., and Kirschner, D. A. (1991) *Biophys. J. 60*, 1190−1201.
51. Mantyh, P. W., Ghilardi, J. R., Rogers, S., DeMaster, E., Allen, C. J., Stimson, E. R., and Maggio, J. E. (1993) *J. Neurochem. 61*, 1171−1174.
52. Paik, S. R., Shin, H. J., Lee, J. H., Chang, C. S., and Kim, J. (1999) *Biochem. J. 340*, 821−828.
53. Esler, W. P., Stimson, E. R., Ghilardi, J. R., Vinters, H. V., Lee, J. P., Mantyh, P. W., and Maggio, J. E. (1996) *Biochemistry 35*, 749−757.
54. Fink, A. L., Calciano, L. J., Goto, Y., Kurotsu, T., and Palleros, D. R. (1994) *Biochemistry 33*, 12504−12511.
55. Ludvigsen, S., Roy, M., Thogersen, H., and Kaarsholm, N. C. (1994) *Biochemistry 33*, 7998−8006.

BI002555C